Available online at www.sciencedirect.com

ScienceDirect

Procedia CIRP 133 (2025) 543–548

www.elsevier.com/locate/procedia

20th CIRP Conference on Modeling of Machining Operations

A simplified numerical model to predict geometrical distortions of thin-walled aluminum airframe components

Aitor Madariaga[a]*, Gorka Ortiz-de-Zarate[a], Zeeshan Yousaf Warraich[a], Pedro José Arrazola[a]

[a]*Mondragon Unibertsitatea, Engineering Faculty, Loramendi 4, 20500, Arrasate-Mondragon, Spain*

* Corresponding author. Tel.: +(34) 664299937; fax: +(34) 943794700. *E-mail address:* amadariaga@mondragon.edu

Abstract

Machined thin-walled airframe components frequently show geometrical distortions due to the alteration of initial bulk residual stresses (IBRS) and machining-induced residual stresses (MIRS) in the final surface. Many authors have proposed numerical models to predict distortions of machined thin-walled components considering the material removal sequence as well as the MIRS. The weight of the component and the boundary conditions also significantly affect the part distortion measurement. Unfortunately, these effects have not been addressed in the literature. This work aims to develop a simplified numerical model to predict geometrical distortions in thin-walled parts. This model does not simulate the material removal process, and IBRS are directly assigned to the final part. The model includes the weight of the part, and an algorithm is proposed to identify the contact points while measuring the part distortion automatically. To validate the model, an aluminum 7475-T7351 part was machined, and geometrical distortions were measured in a coordinate measurement machine under different configurations. These measurement configurations allowed us to address the effect of the weight and boundary conditions on geometrical distortions. The proposed model predicted distortions with a deviation < 15% with respect to experiments and reduced the computational cost by approximately 10 times with respect to the complete model.

Keywords: geometrical distortion; modeling; residual stresses; aluminum alloy

1. Introduction

Aircraft manufacturers compete to produce aircrafts with lower purchase and operation costs demanded by many airline companies [1]. Beyond this context, thin-walled aeronautical monolithic parts made of high strength aluminum alloys with good forming properties enable the manufacturing of lightweight aircraft with increased fuel efficiency [2]. These thin-walled structures are usually obtained by high-speed machining, removing up to 90% of the material from the original plate [3]. Unfortunately, the final component has low stiffness, and the machining process can generate geometric distortions. Part distortion is identified as the form deviation of the final component with respect to the designed part once it has been unclamped [2]. These distortions can generate relevant misalignment and tolerance problems [4], significantly affecting the assembly process and generating pre-stresses that can compromise the in-service behavior of structural components [5]. Although manufacturers meticulously define the machining process to prevent this scenario, frequently out-of-tolerance distortions which require post-processes are generated, or even cause a rejection of the part. For example, based on manufacturing information of four different aircrafts, Boeing estimated that scrap and rework of machined components with geometrical distortions cost the company over 290 million dollars [6].

The distortions of thin-walled monolithic aluminum components are predominantly caused by the initial bulk residual stresses of the material generated in the previous processes (IBRS) and the machining-induced residual stresses

10.1016/j.procir.2025.02.093

(MIRS) [7,8]. It is widely accepted that IBRS greatly impact machining distortion [9]. The distortion is caused by the redistribution of the IBRS that remain within the part rather than the removed material [10]. By contrast, the influence of MIRS is only relevant when the magnitude of IBRS is low and the wall thickness is < 5 mm [11, 12]. Therefore, the main approach to minimize part distortion of monolithic aluminum parts is to control the magnitude and distribution of IBRS and MIRS [3].

Distortion prediction models that include the effect of IBRS and MIRS can be employed to set-up machining strategies that avoid or minimize undesired distortions. Finite element model (FEM) is the most used approach for distortion simulation [9]. Some authors have proposed models that include the IBRS within the initial workpiece and remove the machined material by the element deletion method or including Boolean operation [13-15]. Other authors have used similar approaches but adding MIRS on the final machined surface [12,16] or alternatively simulating the effect of thermal and mechanical loads induced during cutting [17-19].

One of the main disadvantages of those FEM modelling strategies is the high computation cost due to the high number of elements required to model the initial workpiece and the part every material removal step, and in some cases even remeshing. This could be reduced if only the final component is modelled [20], since the part distortion depends on the IBRS that remain in the final part rather than the removed material [10]. Although some authors claim that this simplification comes with an accuracy penalty [9], this inaccuracy has not been addressed in the revised literature.

Additionally, most published works validated the FEM models using components much smaller than thin-walled monolithic structures used in aircraft. In practice, the weight of the component can compensate for the distortion of large components. Furthermore, due to the complexity of the distortion, it is difficult to anticipate the contact points when placing on the coordinate measurement machine (CMM). To the best of the authors knowledge, no published works have included these factors in distortion prediction models.

This work aims to develop a simplified numerical model to predict geometrical distortions in thin-walled parts. The proposed model does not simulate the material removal process, and IBRS are directly assigned to the final part. The model includes the weight of the part, and an algorithm is proposed to automatically identify the contact points while measuring the part distortion. Firstly, the accuracy of the simplified model was assessed by simulating three aluminum 7475-T7351 parts representative of aerostructure components, and comparing to results obtained by the original model that includes the initial part and machining steps. Finally, to validate the model, one of the parts was machined, and geometrical distortions were measured in a coordinate measurement machine under different configurations.

2. Proposed model

The flow-diagram of the proposed model is shown in Fig. 1. This model is based on the simulation strategy developed by Denkena and Dreier [16], and we have added the effect of weight and a novel strategy to define the boundary conditions to identify contact points when measuring the distortion.

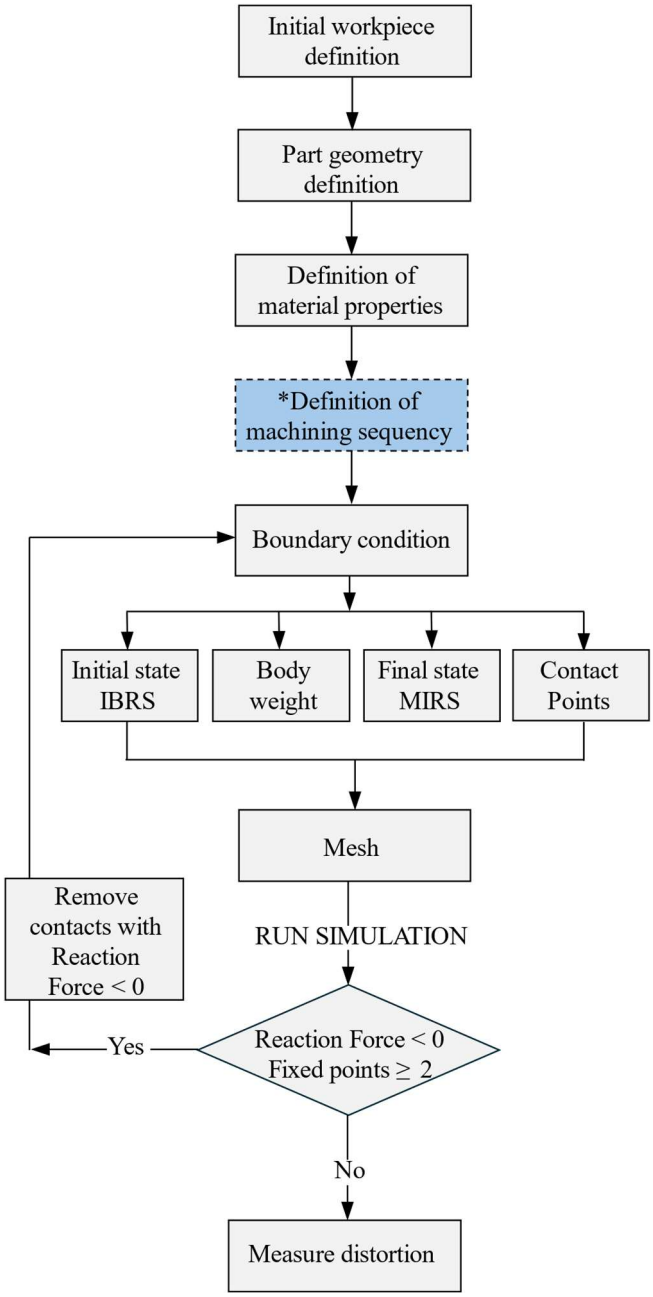

Fig. 1. Flow-diagram of the proposed model.

Firstly, the dimensions of the initial workpiece are defined. Then, the part geometry and its position and orientation within the workpiece are defined. Although the simplified approach does not model the initial workpiece, part position and orientation are key parameters to correctly assign the corresponding distribution of IBRS. Subsequently, mechanical properties and density of the material are defined. It should be clarified that the definition of machining sequence is not necessary for the simplified model, but in case we want to use the original modelling approach, this step should be included. Then, boundary conditions are defined: i) IBRS considering the position and orientation of the part, ii) body weight, iii) MIRS on the final machined surfaces and iv) preliminary contact points for distortion measurement. Finally, the part is meshed

and simulation is launched. Note, that in case we want to apply the original model, the original workpiece must also be meshed. Finally, results are analyzed applying the proposed strategy to identify the contact points of the part when measuring the distortions. Simulations are repeated until the condition for reaction forces (RF) is satisfied.

The approach for identifying correct contact points is schematically shown in Fig. 2. As mentioned above, preliminary contact points (a higher number than expected contact points) are defined. After each simulation, RFs are analyzed in all contact points. If RF < 0, the contact point is removed since it means that the part must be pulled to retain at that point. After *n* iterations, only contact points with RF > 0 will remain, and part distortion will be measured.

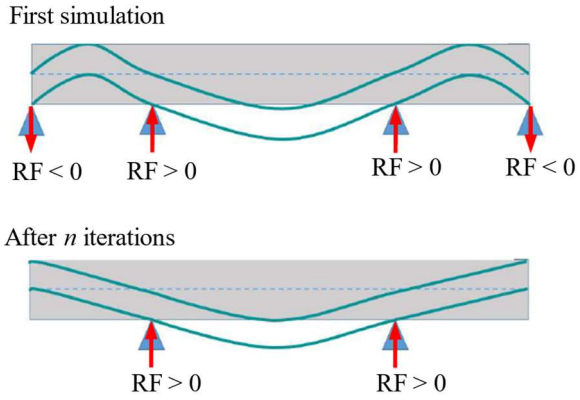

Fig. 2. Approach to identify contact points.

3. Material and experiments

3.1. Material

The specimens employed in this work were cut by abrasive water jet assisted machining from a 40 mm thick aluminum 7475-T7351 plate. Table 1 shows the mechanical properties of the raw material at room temperature in both rolling and transverse direction determined in a previous work [21]. Table 1 shows the Young Modulus (E), yield stress (σ_y), ultimate strength (σ_u) and maximum elongation of the aluminum 7475-T7351 plate. IBRS were characterized in the previous work by the Slitting Method, and details can be found in [21]. They varied from 20 to -35 MPa through the section in the longitudinal direction and from 10 to -15 MPa in the transverse direction. The density of the material is 2800 kg/ m^3.

Table 1. Mechanical properties of Aluminum 7475-T7351 [21].

	Rolling direction	Transverse direction
Young Modulus, E (GPa)	74.2	74
Yield stress, σ_y (MPa)	427	431
Ultimate strength, σ_u (MPa)	530	534
Maximum elongation, (%)	9.5	10.1

3.2. Validation of the simplified model

To experimentally validate the proposed model, the geometry shown in Fig. 3a was designed. It should be noted that the designed geometry had three regions of 50 mm long with more material to intentionally exaggerate the effect of the weight on distortions. Finally, part distortion was predicted using the proposed simplified model. The commercial Abaqus Standard software was employed. The part was meshed using C3D8R type elements with a global nodal distance of 1 mm. The mechanical properties, IBRS and density defined in section 3.1. were applied. The finishing milling conditions used in the experiments were employed in our previous study [21]. These conditions produced very low MIRS (below 50 MPa) within a very thin layer (< 150 µm thick). For this reason, it was assumed that their effect on final distortion would be minor, and MIRS were not included in the simulation. Eight preliminary contact points equally separated along the longitudinal axis were defined, and final contact points were determined in the simulations applying the approach schematically shown in Fig. 2. Two simulations were done: i) without body weight and ii) with body weight.

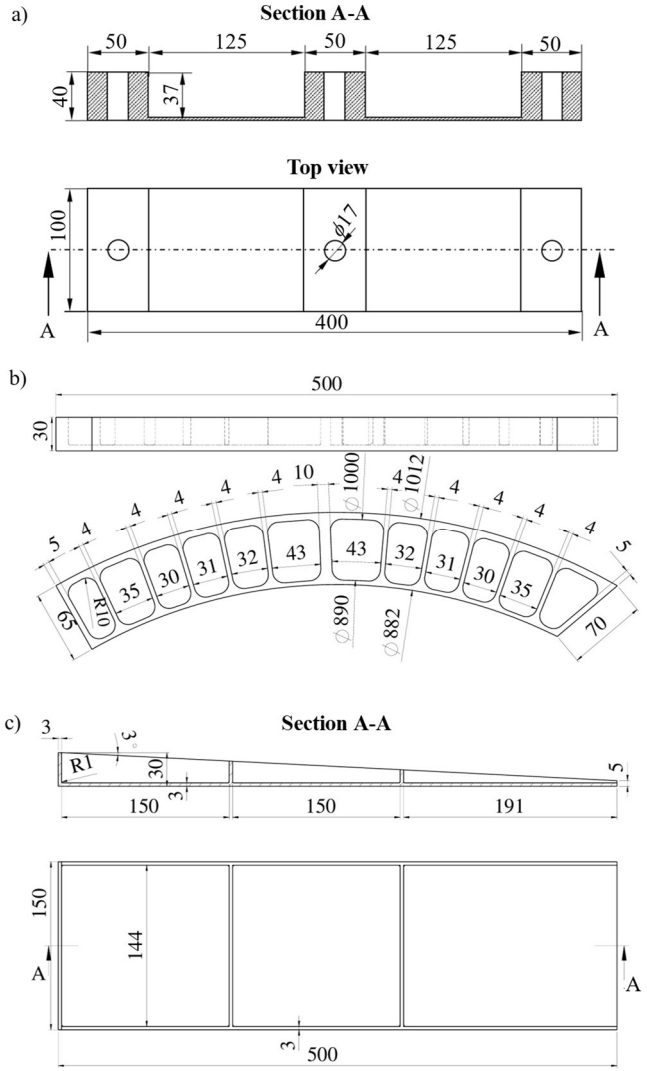

Fig. 3. Geometry of the workpieces to validate the simplified model: a) case study, b) arc shaped part and c) straight part.

The proposed simplified model only models the final part geometry considering the redistribution of IBRS within it. To further test the accuracy of this simplification, two parts representatives of airframe structures were simulated using the complete and simplified model described in section 2. For this comparison, the effect of MIRS was neglected since they are applied to the final geometry and therefore their effect on

distortions is the same for the complete and simplified models. The geometry of the parts is shown in Fig. 3b and 3c respectively. The parts were centered in the thickness of the original workpiece: the flat face of both parts was positioned at 5 mm from the bottom of the original workpiece. Simulations were conducted in commercial Abaqus Standard software, using C3D10 type elements and an average element size of 4 mm, employing the material properties defined in section 3.1.

3.3. Machining experiment and distortion measurement

The geometry defined in Fig. 3a was machined to experimentally validate the proposed model. The workpiece (400×100×100 mm) was cut out from the aluminum 7475-T7351 plate, with the longest side aligned to the rolling direction of the plate. The workpiece was slot milled in the CNC Kondia B1050 machine. The machining sequence consisted of three roughing steps with a depth of cut of $a_p = 12$ mm and the finishing step with $a_p = 1$ mm. The workpiece was clamped with three screws. The cutting speed (v_c), feed per tooth (f_z), and type of cooling used in the experiment are summarized in Table 2. The properties of the uniKENAL 4302.60 tool of 20 mm diameter used in slot milling operation are shown in Table 3.

The distortions of the machined workpiece were measured in a Mitutoyo Crysta-Apex S 7106 CMM. To compare the effect of weight on distortions the machined part was measured using two different orientations as shown in Fig. 4. The main distortion occurred on the z axis. The flat bottom face was in contact with the CMM table to quantify the effect of weight (gravity parallel to z axis) and a total of 20 lines were measured on the machined pockets as can be seen in Fig. 4a. To minimize the effect of weight on part distortion, the part was rotated 90º (gravity perpendicular to z axis), and a total of 8 lines were scanned on the longitudinal direction of the bottom face as shown in Fig. 4b.

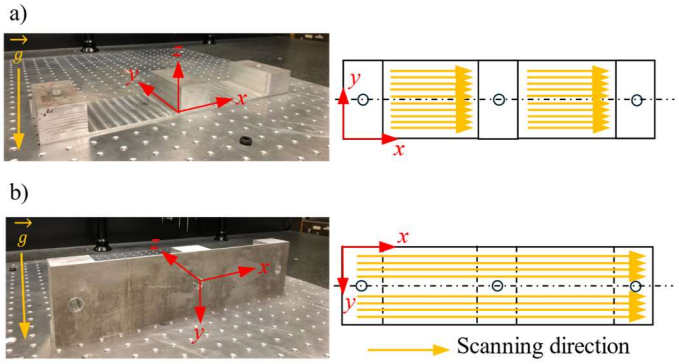

Fig. 4. Orientation of the workpiece on the CMM table and scanning direction to a) consider the effect of weight on main distortion (z axis) and b) neglect it.

Table 2. Cutting conditions used in milling experiment.

	Roughing	Finishing
v_c (m/min)	300	400
f_z (mm/tooth)	0.2	0.2
a_p (mm)	12	1
Coolant	MQL	MQL

Table 3. Properties of the uniKENAL 4302.60 tool.

Material	Uncoated, WC-Co
Diameter (mm)	20
Cutting length (mm)	38
Nose radius (mm)	2.5
Cutting edges (qty)	3

4. Results and discussion

4.1. Numerical validation of the simplified model

Fig. 5 summarizes the simulation process, and the results obtained with the original model and the simplified approach for the three components.

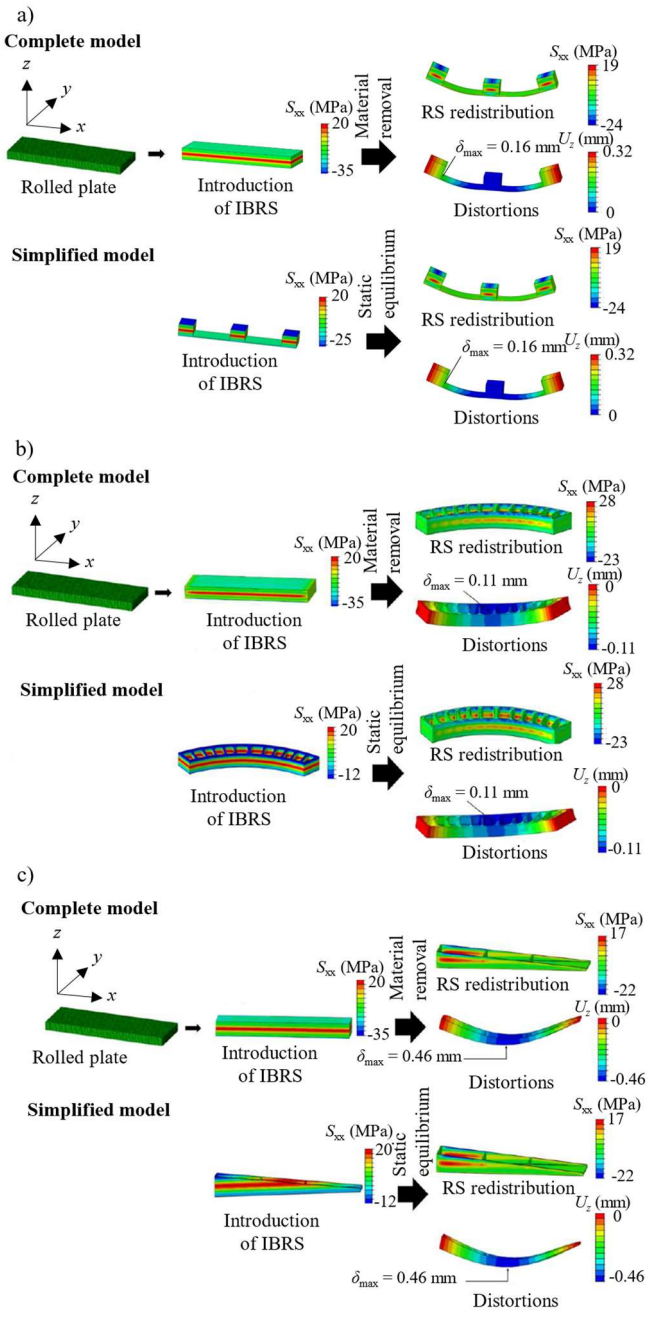

Fig. 5. Simulation process and predicted residual stress redistribution and distortions using the complete and simplified model for the a) case study, b) arc shaped part and c) straight part.

The residual stress distribution (S_{xx}, residual stresses parallel to the rolling direction) on the final geometry of the tested cases is the same for the complete and simplified models as can be seen in Fig. 5. Similarly, all models predicted the same distortion and maximum deflection of the part: δ_{max} = 0.16 mm for the case study, δ_{max} = 0.11 mm for the arc shaped part, and δ_{max} = 0.46 mm for the straight part. Therefore, this confirms that the final redistribution of IBRS does not depend on the removed material but on the part geometry and its position in the initial plate [10].

These simulations were done using a Workstation with 8 core processors. The computational cost was significantly reduced when using the simplified model compared to the complete model. For the arc shaped part, it was 9 times lower, and for the straight part 10 times lower. It can be concluded that the simplified model does not compromise the accuracy of the model and significantly reduces the computation cost.

4.2. Experimental results: effect of weight and validation of the model

Fig. 6 compares the experimentally and numerically measured distortions in the *z* axis of the machined part (see Fig. 4 for reference) considering the effect of weight and without it. As described in section 3.2 the part geometry was designed to increase the effect of weight. The maximum distortion was reduced from 0.4 mm to 0.14 mm when considering the effect of weight on the experiments. Similarly, the simplified model predicted a reduction from 0.45 mm to 0.16 mm. On average, both experiments and simulations found a distortion reduction of 65%. It should be clarified that this significant reduction cannot be generalized since the workpiece was designed to exaggerate the effect of weight, and the effect of MIRS was minimized by the selected cutting conditions. Nevertheless, these results evidence that part weight must be included in distortion prediction models when measuring the distortion, and this might be particularly relevant in large components with low stiffness.

The simplified model and experiments measured the same distortion shape as can be seen in Fig. 6. The central region of the part was in contact with the CMM table when considering the effect of weight on distortion. The simplified model was defined with 8 preliminary contact points equally spaced along the *x* axis as described in section 3.2. The proposed model, after several iterations, removes the preliminary contact points that will not be in contact due to the residual stress distribution (see Fig. 2). Since both experiments and simulations obtained the same distortion shape, it can be concluded that the approach to identify contact points when measuring the part distortion on the CMM table is valid.

Regarding the accuracy of results, the simplified model predicted the maximum distortion with an error of approximately 15% in all cases. Multiple factors could have contributed to these errors: i) IBRS were characterized in a previous work [21] using a limited number of samples and ii) the characterized profiles were considered uniform throughout the entire aluminum 7475-T7351 plate. It is very likely that IBRS vary throughout the plate; therefore, the uniformity assumption applied in the numerical model can lead to errors. It must be clarified that the current state of the art of residual stress measurement technology does not allow us to measure non-destructively the entire residual stress distribution of a large component. Therefore, the error provided by this assumption is within the acceptable range. The other possible error source is the effect of MIRS. The magnitude and affected layer were low for the applied finishing conditions, and their influence on final distortion should have been minor.

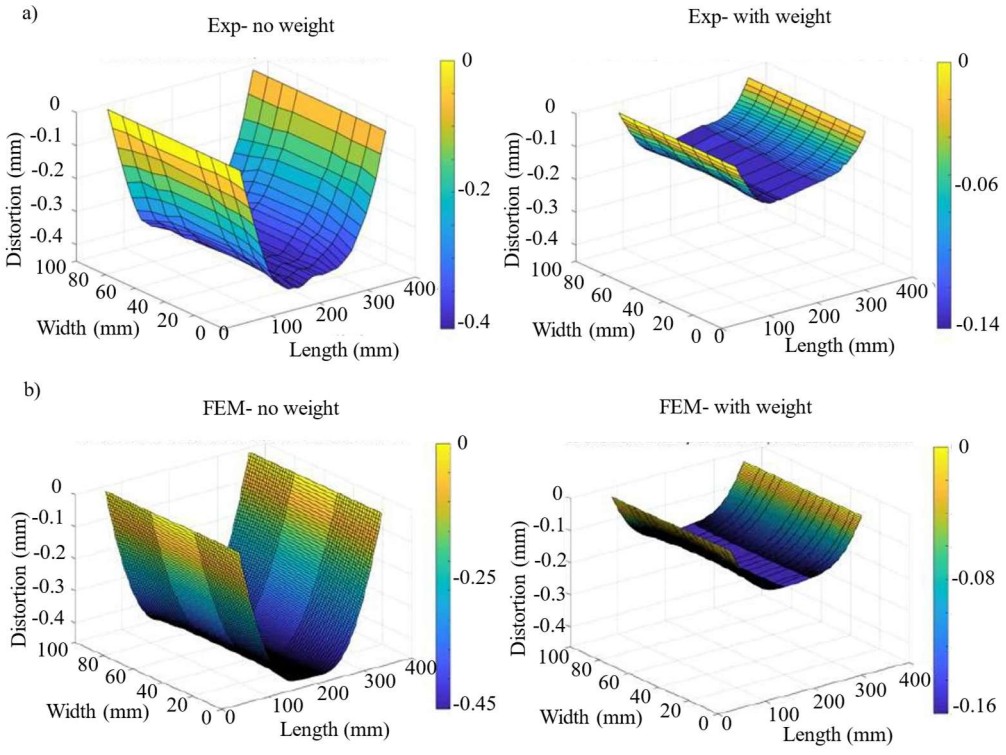

Fi g. 6. a) Experimentally and b) numerically determined distortions considering the effect of weight and neglecting it.

5. Conclusions

This work is aimed at developing a simplified numerical model to predict geometrical distortions in thin-walled parts. The main conclusions are:

- A simplified model that only considers the final component geometry, its position, and orientation within the initial workpiece accurately predicts the effect of distortions on final distortion. This model also confirms that the effect of IBRS depends on the redistribution within the final component rather than the relaxation of IBRS of the material removed during machining. The simplified model can reduce 10 times the computational cost required by the complete simulation strategy that includes the original workpiece and all machining strategies.
- The effect of weight on part distortion can be relevant and this must be included in the FEM models to predict part distortion. For the tested conditions, the weight significantly reduced the distortion by 65%, but this cannot be generalized since its effect depends on the part material and geometry.
- The approach for identifying the real contact points when measuring the distortion on the CMM table was validated. This approach defines preliminary contact points and removes non-valid ones by verifying the reaction force.

Acknowledgements

The authors thank the Basque Government for the financial support given from Elkartek Program to the project NG24 – *Desarrollos en la nanoescala para procesos avanzados de fabricación de metales* (KK-2024/00001), as well as the grant IT 1443-22 given to the research group within the Program to support the activities of research groups of the Basque university system. The authors also acknowledge the Ministerio de Ciencia e Innovación of the Spanish Government for the funding given to TAILORSURF project (PID2022-139655OB-I00).

References

[1] Dursun T, Soutis C. Recent developments in advanced aircraft aluminium alloys. Mater Des 2014; 56:862-71.

[2] Sim WM (2009) Residual stress engineering in manufacture of aerospace structural parts. Filton, UK: Airbus SAS. [Internet] 2009 [cited 20-09-2017], Available from: www.transport-research.info Accessed 20 September 2017

[3] Li JG, Wang SQ. Distortion caused by residual stresses in machining aeronautical aluminum alloy parts: recent advances. Int J Adv Manuf Technol 2017; 89(1):997-1012.

[4] Costa MI, Leitão C, Rodrigues DM. Parametric study of friction stir welding induced distortion in thin alu-minium alloy plates: A coupled numerical and experimental analysis. Thin-Walled Struct 2019;134:268-76.

[5] Zhang L, Wang H, Li S. Simulating assembly geometric and stress variation considering machining-induced residual stress. In International Design Engineering Technical Conferences and Computers and Information in Engineering Conference; 2014 August 14-17; Buffalo, USA: ASME 2014;46353;V004T06A011.

[6] Bowden DM, Halley JE. Aluminium reliability improvement program-final report 60606. Chicago, IL, USA: The Boeing Company 2001.

[7] Wang ZJ, Chen WY, Zhang YD, Chen ZT, Qiang LIU. Study on the machining distortion of thin-walled part caused by redistribution of residual stress. Chin J Aeronaut 2005;18(2):175-9.

[8] Li Y, Gan W, Zhou W, Li D. Review on residual stress and its effects on manufacturing of aluminium alloy structural panels with typical multi-processes. Chin J Aeronaut 2023;36(5):96-124.

[9] Aurrekoetxea M, Llanos I, Zelaieta O, López de Lacalle LN. Towards advanced prediction and control of ma-chining distortion: a comprehensive review. Int J Adv Manuf Technol 2022;122(7-8),2823-48.

[10] Yang Y, Fan L, Li L, Zhao G, Han N, Li X. Tian H, He N. Energy principle and ma-terial removal sequence optimization method in machining of aircraft monolithic parts. Chin J Aeronaut 2020;33(10),2770-81.

[11] Akhtar W, Lazoglu I, Liang SY. Prediction and control of residual stress-based distortions in the machining of aerospace parts: A review. J Manuf Process 2022;76,106-22.

[12] Weber D, Kirsch B, Chighizola CR, Jonsson JE, D'Elia CR, Linke BS, Hill MR, Aurich JC. Investigation on the scale effects of initial bulk and machining induced residual stresses of thin walled milled monolithic aluminum workpieces on part distortions: experiments and finite element prediction model. Procedia CIRP 2021;102,337-42.

[13] Chantzis D, Van-der-Veen S, Zettler J, Sim WM. An industrial workflow to minimise part distortion for ma-chining of large monolithic components in aerospace industry. Procedia CIRP 2013;8,281-6.

[14] Zhang Z, Li L, Yang Y, He N, Zhao W. Machining distortion minimization for the manufacturing of aeronau-tical structure. Int J Adv Manuf Technol 2014;73, 1765-73.

[15] Cerutti X, Mocellin K. Influence of the machining sequence on the residual stress redistribution and ma-chining quality: analysis and improvement using numerical simulations. Int J Adv Manuf Technol 2016;83,489-503.

[16] Denkena B, Dreier S. Simulation of residual stress related part distortion. In Denkena B editors. New Produc-tion Technologies in Aerospace Industry: Proceedings of the 4th Machining Innovations Conference;2013 September; Hannover, Germany. Berlin: Springer International Publishing; 2013. 105-13.

[17] Tang ZT, Yu T, Xu LQ, Liu ZQ. Machining deformation prediction for frame components considering multifactor coupling effects. Int. J. Adv. Manuf. Technol 2013;68(1-4):187-96

[18] Hussain A, Lazoglu I. Distortion in milling of structural parts. CIRP Annals 2019;68(1):105-108.

[19] Akhtar W, Lazoglu I. A novel hybrid model for prediction of distortions in milling. CIRP Annals 2023;72(1):73-76.

[20] Marusich TD, Usui S, Marusich KJ (2008) Finite element modelling of part distortion. Intelligent Robotics and Applications. Springer, Berlin Heidelberg, Berlin, Heidelberg, pp 329–338

[21] Madariaga A, Cuesta M, Ortiz-De-Zarate G, Sáenz-De-Argandoña E, Soriano D, Prime MB, Arrazola PJ. Correcting distortions of thin-walled machined parts by machine hammer peening. Chin J Aeronaut 2024;37(6):439-53